NONDESTRUCTIVE DIAGNOSTICS FOR MEASURING THE PHASE, POSITION, AND INTENSITY OF 15 enA BEAMS FROM THE IUCF CYCLOTRON

Timothy J. P. Ellison, C. Michael Fox, Steven W. Koch
Indiana University Cyclotron Facility, 2401 Milo B. Sampson Lane, Bloomington, IN 47405, USA

Liu Rui
Institute of Modern Physics, Academia Sinica, P.O. Box 31, Lanzhou, Peoples Republic of China

Abstract

Nondestructive rf beam diagnostics, designed for use in the IUCF Cooler storage ring, are now in use in the cyclotron beam lines. Wall gap monitors are used to monitor the beam microscopic time structure, macroscopic time structure, and phase with respect to the main synthesizer; electrostatic pick-up electrodes are used to monitor the beam position and intensity. These monitors were designed to operate with beam intensities ranging from 10 nA to 10 μA. Simple models and equivalent circuits are given for each pick-up, and the electronics used to measure beam properties are described. For each type of pick-up the signal and noise voltages are calculated; methods to eliminate coherent and incoherent noise are discussed.

Introduction

Nondestructive rf diagnostics have long been used in synchrotrons, where the interceptive diagnostics used in single-pass machines would destroy the beam before a measurement could be made. Single-pass machines, however, have traditionally used interceptive devices such as wire scanners and Faraday cups because noninterceptive devices are not usually required and, since cyclotrons generally operate with much lower beam currents than synchrotrons, rf pick-ups are much more difficult to implement. Rf pick-ups, however, nicely complement interceptive diagnostics and allow measurement of beam properties which are otherwise difficult to make. For example, a wall gap monitor can measure the intensity of a 15 enA cyclotron beam with a 1 kHz bandwidth (BW) and an rms signal-to-noise ratio (S/N) of about 30 dB; electrostatic pick-up electrodes can monitor the position of a 15 nA beam at a polarimeter or target with a bandwidth of 0.1 Hz and an rms signal-to-noise ratio of about 40 dB without adding any background to the experiment.

The Wall Gap Monitor and Its Uses

Wall Gap Monitor Design.

The wall gap monitor directly measures the beam ac current. Figure 1 shows a schematic and equivalent circuit model for a wall gap monitor, as well as the circuit element values for the IUCF monitors. A wall gap monitor can be viewed as a single 1:1 transformer, with the beam acting as the primary winding and the vacuum chamber as the secondary; alternatively, as a device which forces the wall current (approximately the negative image of the beam current) through an external monitoring resistor.[1] The capacitance across the gap, and the inductance of the two EMI copper shields, are shown in the equivalent circuit.

Bandwidth. The low frequency 3 dB point (radians/s) is R/L, and the high frequency 3 dB point is 1/RC. For frequencies within this range, the impedance of the pick-up is approximately R, and the phase shift is approximately constant and equal to 0. The bandwidth of the monitor can be easily extended by decreasing R at the expense of decreasing the S/N. The IUCF monitors use low noise amplifiers with an input impedance of 50 Ω.

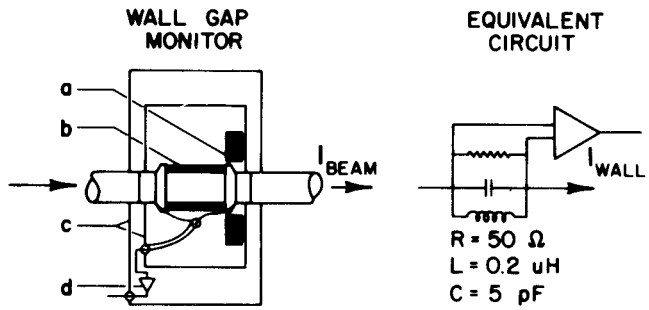

Fig. 1. Design and equivalent circuit for a wall gap monitor: a) ferrite toroid; b) ceramic insulator; c) copper EMI shields; d) low noise amplifier.

Signal and Noise Voltages. The amplitude of the amplifier input signal voltage is simply $K(\omega)IR$ if ω is within the bandpass of the pick-up. I is the dc beam current, ω the radial frequency, R the amplifier input impedance, and $K(\omega)$ the coefficient of the Fourier component of the normalized beam current at the frequency ω. For cyclotrons with narrow phase acceptances, such as the IUCF cyclotron,[2] the beam can be modeled as a repetitive delta function, and $K(\omega)$ is simply equal to 2 for all frequencies which are an integer multiple of the fundamental frequency.

The amplifier input noise voltage is determined by the amplifier noise figure, and is proportional to the square root of the bandwidth in Hz. (The noise BW is not the same as the 3dB BW. For example, the noise BW is 1.57 times the 3 dB BW for a single pole filter).[3] The noise voltage will be increased by another factor of $\sqrt{2}$ if image rejection mixers are not used in the signal processing electronics. The noise is Gaussian and the peak-to-peak voltage noise is defined here as 8 times the standard deviation (rms) value. The actual voltage fluctuations will be less than this value 99.994% of the time. Low noise high bandwidth 50 Ω amplifiers with input noise voltages of less than 0.6 nV $\sqrt{\text{Hz}}$ are commercially available from many vendors.

The IUCF wall gap monitors have a BW of about 1000 MHz. When viewed on a 300 MHz bandwidth oscilloscope, the noise voltage is approximately 13 μV (rms), which is the voltage produced by about 460 nA of beam current. The peak S/N observed is much better than this because the beam comes in very short pulses, as shown in Fig. 2.

Beam Amplitude Monitor.

In order to increase the S/N, it is necessary to build a narrow filter which allows the signal through, but filters out the surrounding amplifier noise. Since

it is impractical to build a sufficiently narrow (e.g. 100 Hz wide) filter at 30 MHz, synchronous detectors are used. The simplest type of synchronous detector is shown in Fig. 3. The output signal at the IF port of the mixer (phase detector) is proportional to the product of the signals at the rf port (RF) and the local oscillator (LO) port of the mixer. After

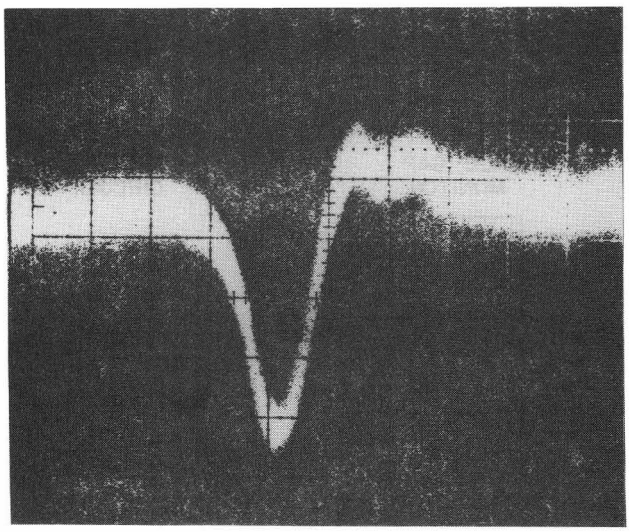

Fig. 2. The output of an IUCF wall gap monitor viewed on a 300 MHz scope. The average beam current was 25 nA, and the pulse repetition period 100 nS.

low-pass filtering, the output voltage is proportional to the amplitude of the beam signal times the cosine of the phase angle between the two input signals. The output of such a monitor, built at IUCF, is shown in Fig. 4. There are two major problems with a monitor of this type: The phase of the local oscillator signal must be adjusted, and there are large dc offsets which change with time. Both of these problems are overcome by mixing to an intermediate frequency (IF) other than dc by offsetting the local oscillator frequency from the beam frequency. This technique is used in the beam position monitor electronics which are described below.

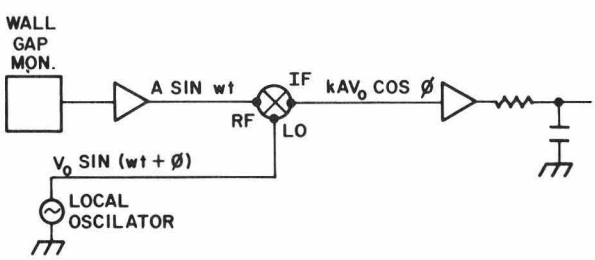

Fig. 3. Schematic of a simple synchronous detector.

Beam Phase Detector.

Figure 5 is a simplified schematic for the beam phase detector which uses the signal from a wall gap monitor. Figure 6 shows the timing accuracy of this monitor as a function of beam current. The performance of this detector is limited at low currents by the high, approximately 200 kHz bandwidth of the IF section in the HP 8405A vector voltmeter. The beam position electrode electronics, described below, have IF

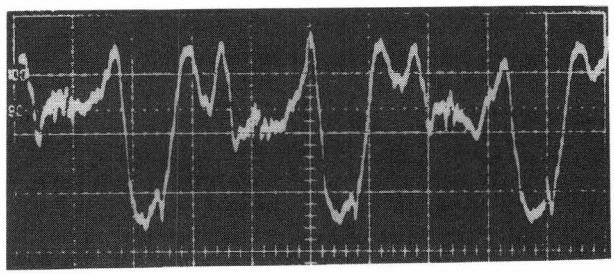

Fig. 4. The output of a simple beam amplitude monitor similar to Fig. 3, for an average beam current of 15 nA. (7 nA/div vertical; 5 ms/div horizontal). The line frequency (60 Hz) modulation of the beam current is very apparent, and not easily observable using more standard beam current measurement techniques.

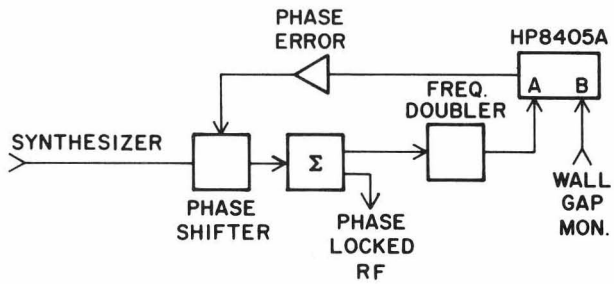

Fig. 5. Block diagram of the beam phase detector used at IUCF as a timing reference for experiments.

bandwidths of only 10 or 100 Hz. In the future, we plan to modify one of these detectors to operate as a phase detector to replace the HP 8405A, thus extending the accuracy of this monitor to lower beam currents.

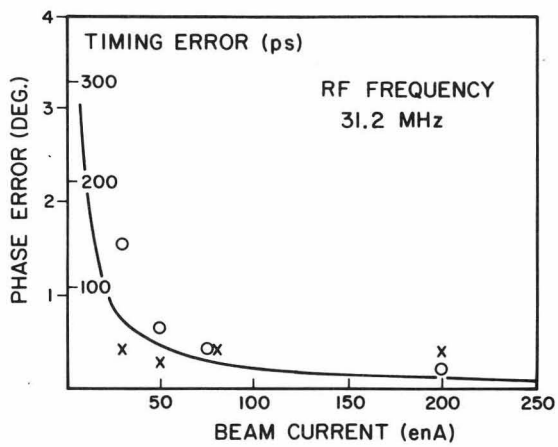

Fig. 6. Timing accuracy of the beam phase detector. The solid line is the maximum error that might occur due to interference from the rf systems. The open circles represent the peak-to-peak error due to amplifier noise, and the crosses the drift with time. The rf pick-up (solid curve) was eliminated by moving the wall gap monitor about 10 meters away from the cyclotron.

Methods of Eliminating RF Noise

The amplifier noise can be reduced to arbitrarily small values by filtering. However, since the rf noise from the accelerator rf systems is usually at exactly the same frequency as the beam signal, no amount of filtering can increase the S/N(rf). After all methods of rf shielding have been tried, and failed to provide sufficient S/N, there is still hope. First of all, for cyclotron beams with narrow phase widths, the beam power at harmonics of the fundamental frequency is about the same as at the fundamental frequency, while most of the rf interference is at the fundamental frequency. Measurements made at higher harmonic numbers have increased S/N. The IUCF phase detector system operates on the second harmonic of the cyclotron rf frequency.

An even more powerful technique is to pulse-select the beam. At IUCF, the cyclotron can be easily operated so that there is a beam pulse only every other rf cycle, by using bunchers which operate at both the frequency of the cyclotron rf systems, and at half that frequency. This method of bunching actually increases the average beam current, because the bunching is more efficient than in the non-pulse-selected mode. Now there are approximately equal amounts of beam power at every harmonic of half the rf frequency, but all the interference comes only at harmonics of the rf frequency. The IUCF beam position monitor system operates at 3/2 the rf frequency with beams that are pulse-selected 1 in 2n, where n is an integer, with no measurable rf interference.

The IUCF Beam Position Monitoring (BPM) System

Electrodes.

As with wall gap monitors, electrostatic pick-ups have been around for longer than anyone can remember. Figure 7 shows a schematic and equivalent circuit for the beam position electrodes. The aluminum electrodes used in the IUCF cyclotron beam lines have a length (L) of 10 cm, diameter of 6 cm, and are housed in a vacuum chamber with a 10 cm inner diameter. With the feedthrus, cables, and amplifiers attached, the total capacitance per electrode (C) is 35 pF, and the coupling capacity between the two electrodes (C_c) is about 5 pF.

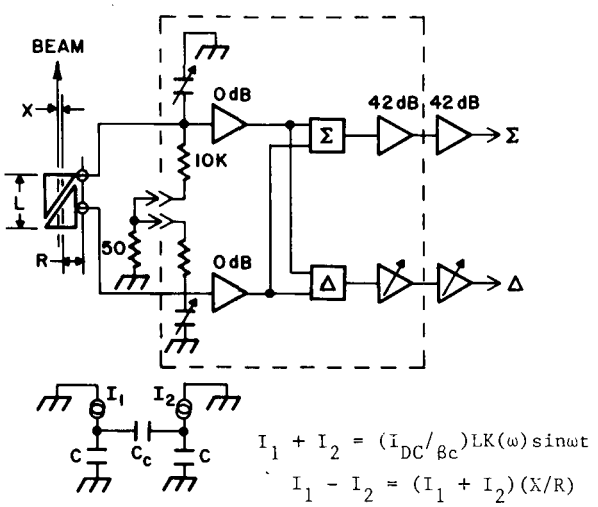

Fig. 7. Schematic of, and equivalent circuit for, a beam position electrode, and block diagram of electrode amplifiers.

Signal and Noise Voltages. Whereas wall gap monitors are sensitive to the beam current, BPM electrodes are sensitive to the beam linear charge density, or the beam current divided by velocity (βc). If the amplifier input resistance (R) is much greater than $1/\omega C$, negligible amounts of charge will flow through the input resistor. Assuming for now that there is just one cylindrical electrode, which is equivalent to assuming that the beam is centered, the voltage seen at the input of each amplifier is simply the charge contained within the electrode divided by 2C. If the electrode is much shorter than the beam wavelength, $\beta c/\omega$, we can approximate the total charge as the linear current density times the length of the electrode: $K(\omega)IL/\beta c$. Therefore the voltage is simply $K(\omega)IL/2\beta cC$. Alternately, one can take the time derivative of the charge ($K(\omega)\omega IL/\beta c$) and apply this current across the electrode impedance ($1/2\omega C$).

The FET input amplifier noise is about 2.8 nV/√Hz. When signals from each amplifier are added together in the power combiners, the signal voltages add coherently, while the noise voltages add incoherently. This yields an effective coupling impedance of $K(\omega)L/\beta cC$, or about 16 Ω for the IUCF system parameters with $\beta = 0.57$, and an effective input noise of about 4 nV/√Hz. Comparing these values with those obtained for the wall gap monitors, we see that the S/N is about 20 times lower for the position electrodes. However, since the signal on the electrodes is inversely proportional to the beam velocity, for very low energy beams ($\beta < 0.03$) they are superior to the wall gap monitors in terms of S/N.

Electrode Linearity. Suppose the coupling capacity between the two electrodes is zero. Then the difference between the currents from the two electrodes, divided by the sum of these currents, is x/R, where x and R are defined in Fig. 7. This can be easily demonstrated for a parallel plate geometry using Green's reciprocity theorem.[4] With more difficulty, it can be shown that this is also true for rectangular and cylindrical electrodes. In many cases it may be most easily shown through experiment. Generally the electrodes are the two halves of a cylinder split diagonally, as in Fig. 7, so that they are only sensitive to beam movement in one direction.

With non-zero coupling capacity C_c, the difference between the currents from the two electrodes, divided by their sum, is Ax/R, where A is $C/(C + 2C_c)$. This can be easily shown by applying all the current to one electrode and using Kirchoff's laws to solve for the voltage.

Beam Position Electrode Amplifiers

A block diagram for BPM electrode amplifiers is shown in Fig. 7. Elantec EL2004C FET-input buffer amps are used to sense the electrode voltages. Each amplifier input is connected through a 10 k Ω resistor to a common 50 Ω resistor to ground, giving the amplifiers a low frequency 3 dB point of about 0.5 MHz. The 10 k Ω resistors were matched at dc to better than 10 Ω (0.1%). At frequencies up to 20 MHz they still are matched to within 1%, which is the precision with which we can measure rf voltages. When an rf voltage source is applied to the 50 Ω resistor to ground, the 10 k Ω resistors act as calibration current sources for the amplifiers, and the offset for centered beam can be measured. The sensitivity (Volts/I·mm), which is influenced by the coupling capacity between the two electrodes, can be measured by applying voltage to only one calibration input.

Adjustable input capacitors on each channel allow balancing of the two input channels, compensating for

differences in capacitance or FET amplifier gain. By adjustment of these capacitors, the common mode rejection for the difference amplifier can be made almost arbitrarily high at any one frequency. Certain amplifiers tested have a CMRR of greater than 60 dB from 1 to 40 MHz.

The vector sum and difference of the two voltages are produced using power combiners, and then amplified twice by 42 dB before being sent back to the control room. This large amount of amplification, together with the fact that we operate on the 3/2 harmonic of the cyclotron rf frequency, allows us to use relatively inexpensive cable (RG-58) to transmit the signals with negligible rf interference.

The 42 dB amplifiers have a 10 dB adjustment range. This allows us to give dissimilar electrodes similar effective impedances and sensitivities. The amplifier upper 3 dB point is 80 MHz, limited by the input buffers. The equivalent input noise voltage is constant to within 1 dB over this range.

Position Detector Electronics

A block diagram of this detector, which generates output voltages proportional to the position and intensity of the beam at the position electrode pair, is shown in Fig. 8. Detailed schematics and further information can be obtained by contacting any of the authors. The detector offset error divided by the full scale output voltage range is less than 0.1% over a dynamic range of 63 dB, which corresponds to beam currents ranging from 10 nA to 14 μA. Since the peak noise voltage (defined here as 4 times the rms value) remains greater than the peak signal voltage for currents ranging from 10 nA to 10 μA, rf gain switching is pointless. The beam position detector electronics, however, has an automatic 20 dB gain switch in the IF section.

The detector, which uses the amplitude to phase conversion scheme[5] for determining beam position, was modeled after the low bandwidth beam position detectors built at FNAL for the Antiproton Source.[6] The IUCF detector, however, was designed to work with lower beam currents and has a lower IF frequency (2.777 kHz) and lower IF BW (100 Hz), which limits the output bandwidth to 50 Hz. The output signal is then put through an additional filter to further reduce the noise. At very low beam currents (10 nA), a 0.1 Hz lowpass filter is needed to get sufficient S/N. However, with high beam currents (10 μA), a peak-to-peak S/N of about 60 dB can be obtained with a 50 Hz output bandwidth. Therefore, a single pole, continuously-adjustable, voltage-controlled lowpass filter, whose 3 dB point can vary from 0.1 to 50 Hz, was installed on the output. The pole frequency is proportional to the intensity signal, which is derived in this same detector. Thus the S/N increases with the 1/2 power of the beam current. The pole position modulation bandwidth is 100 Hz, and thus the filter functions somewhat like a sample-and-hold amplifier during short beam interruptions. The variable filter is followed by a fixed 50 Hz filter. The result of all this filtering is shown in Fig. 9.

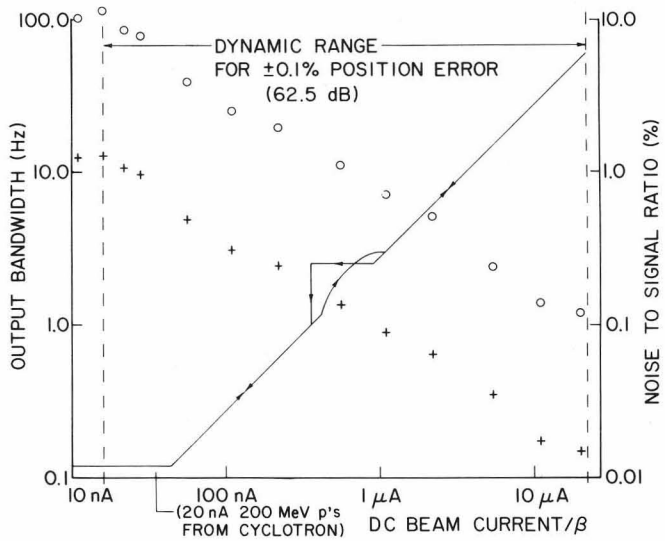

Fig. 9. Plot showing the bandwidth (solid line), and measured rms (crosses) and peak-to-peak (open circles) noise-to-full-scale-signal-voltage ratios for the beam position monitor system as a function of beam current. The effect of coupling capacitance has been neglected.

The position and intensity signals from these detectors are fed into the PDP 11/44 control computer. Closed-loop steering programs have been written to stabilize the beam position, using these detectors and electrodes installed in front of the polarimeters in beamlines 4 and 5. In several tests, this system has proven to be effective in stabilizing the beam position against variations lasting longer than about three seconds. With 50 nA of beam current, the peak-to-peak deviation of the BPM position signal over a period of one-half hour, using the 0.1 Hz filter, corresponded to a peak-to-peak beam position movement at only 0.3 mm at the electrodes. A considerable part of this position

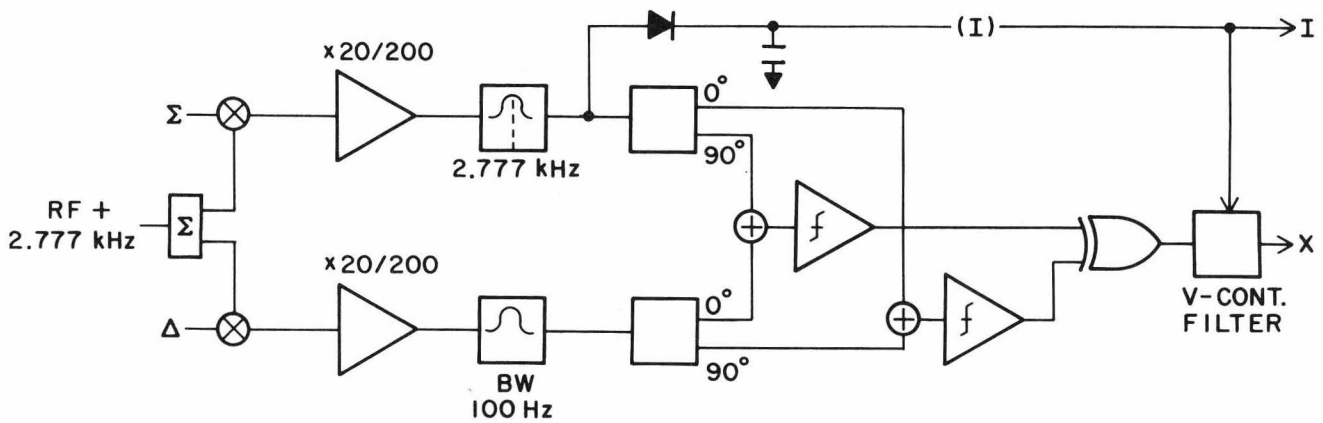

Fig. 8. Block diagram of beam position detector electronics.

signal deviation was due to amplifier noise, rather than actual beam movement. Further testing is necessary to determine the longer-term stabilization capabilities of the system.

Summary

In the next year, although most of our work will be on Cooler diagnostics, we hope to improve the phase probe for operation at lower beam intensities, commission the steering loop programs, and install a buncher phase modulator to eliminate the line frequency modulation of the beam current, thereby increasing the average intensity.

Acknowledgements

Many thanks to John Collins, who wrote the software for the closed loop steering programs, and to the operations staff at IUCF for their valuable help.

This work was supported by NSF Grants NSF PHY 82-11347 and NSF PHY 84-12177.

References

1. R. Littauer, AIP Conf. Proc. No. 105 (1983).
2. R.E. Pollock, IEEE Transactions on Nuclear Science. NS-24, 1505 (1977).
3. R. Pettai, Noise in Receiving Systems, John Wiley and Sons, NY (1984), p.37.
4. J. D. Jackson, Classical Electrodynamics, 2nd Ed., John Wiley & Sons, Inc., NY (1975), p. 51, Problem 1.12.
5. R. E. Shafer and R. E. Gerig, Proc. of 12th Int. Conf. on High Energy Accel. (Fermilab, 1983), pg. 609.
6. T. Bagwell et al, FNAL TM-1254 (1984) (unpublished).